Journal of Alloys and Compounds 834 (2020) 155018

Contents lists available at ScienceDirect

Journal of Alloys and Compounds

journal homepage: http://www.elsevier.com/locate/jalcom

$CoFe_2O_4$-filled carbon nanotubes as anode material for lithium-ion batteries

Lucas Möller [a], Elisa Thauer [a, *], Alexander Ottmann [a], Lukas Deeg [a], Rasha Ghunaim [b, c], Silke Hampel [b], Rüdiger Klingeler [a, d, **]

[a] Kirchhoff Institute of Physics, Heidelberg University, INF 227, 69120, Heidelberg, Germany
[b] Leibniz Institute for Solid State and Materials Research (IFW) Dresden, Helmholtzstraße 20, 01069, Dresden, Germany
[c] Department of Applied Chemistry, Palestine Polytechnic University, Hebron P.O. Box 198, Palestinian Territories, Germany
[d] Centre for Advanced Materials (CAM), Heidelberg University, INF 225, 69120, Heidelberg, Germany

ARTICLE INFO

Article history:
Received 30 January 2020
Received in revised form
31 March 2020
Accepted 1 April 2020
Available online 5 April 2020

Keywords:
Lithium-ion batteries
Carbon nanotubes
Cobalt ferrite
Anode material
Nanocomposite

ABSTRACT

Nanosized particles of cobalt ferrite $CoFe_2O_4$ incorporated into multi-walled carbon nanotubes (CNT) have been studied as anode material for Li-ion batteries. In order to evaluate the benefits of CNT shells, the results are compared to bare $CoFe_2O_4$ nanoparticles. Electrochemical measurements by means of cyclic voltammetry and galvanostatic cycling show typical redox activity associated with the ferrite conversion reaction which implies that the filled nanomaterial is electrochemically active. Galvanostatic cycling measurements reveal better cycling stability of the CNT-incorporated compared to the bare ferrite nanoparticles. The data imply that embedding nanoparticles inside the protective and conductive shells of CNTs opens a way to utilize high theoretical capacities of $CoFe_2O_4$ for electrochemical energy storage.

1. Introduction

First row transition metal oxides have been known to be promising materials for energy storage in lithium ion batteries (LIBs) [1,2]. This is due to their large theoretical specific capacities based on conversion mechanisms involving the reduction to their metallic constituents and Li_2O [3]. One of these promising conversion materials is the here studied spinel-structured cobalt ferrite $CoFe_2O_4$ which exhibits a theoretical capacity as large as 914 mA h g^{-1} if full conversion to Co and Fe is assumed, i.e., insertion of 8 Li^+/f.u. However, $CoFe_2O_4$ suffers from typical drawbacks of oxide conversion materials such as bad conductivity [4] and large volumetric changes upon the reaction with lithium [1,5]. This causes mechanical degradation of the materials including its electrical insulation and associated poor cycle life. The resulting capacity losses upon electrochemical cycling are the main reason that $CoFe_2O_4$ cannot be utilized as an electrode material in LIBs, yet. One approach to overcome the material's drawbacks has been the fabrication of nano-porous morphologies, thereby compensating for volumetric changes as well as improving the ionic conductivity [6,7]. The impact of porosity on the cycling stability has been demonstrated, e.g., by Fu et al. [8]. Highly improved reversible capacities have been reported for thin films [9], nanorods [10], and nanospheres [11], among others [12–14]. Another approach employs embedding of the ferrite material inside highly conductive carbon matrices in order to prevent $CoFe_2O_4$ from becoming electrically insulated. Successful attempts have been done by using $CoFe_2O_4$/C-fibers [15], coated graphene sheets [16], reduced graphene oxide composites [17] and coated carbon nanotubes [18,19]. For this work, a composite of $CoFe_2O_4$ and multi-walled carbon nanotubes (CNTs) is created by filling CNTs with iron and cobalt nitrite and subsequent conversion of the filling to $CoFe_2O_4$. Encapsulation of functional fillings into CNT for improving the stability is a known strategy to obtain improved materials properties. It is widely used and finds application in various fields such as electrocatalysis [20,21], magnetic data storage technologies [22,23], nanomedicine [24,25], and sensors for magnetic force microscopy [26]. Here, it is exploited to obtain a $CoFe_2O_4$ nanoparticle-based

* Corresponding author.
** Corresponding author. Kirchhoff Institute of Physics, Heidelberg University, INF 227, 69120, Heidelberg, Germany.
E-mail addresses: elisa.thauer@kip.uni-heidelberg.de (E. Thauer), klingeler@kip.uni-heidelberg.de (R. Klingeler).

https://doi.org/10.1016/j.jallcom.2020.155018
0925-8388/

material where the active nanomaterial is wrapped by the protective carbon-shells of CNT which form a conducting network [27–29]. The electrochemical performance of cobalt ferrite incorporated in CNTs ($CoFe_2O_4$@CNT) is investigated and compared to that of bare $CoFe_2O_4$ nanoparticles.

2. Experimental

2.1. Synthesis of filled CNTs

Multi-walled carbon nanotubes of the type PR-24-XT-HHT (Pyrograf products) have been used as template for filling them with cobalt ferrite. The filling procedure is an extension of a reported solution based filling approach for CNTs with $ZnFe_2O_4$ [30]. 1 M standard aqueous solutions of the following nitrates have been prepared: $Fe(NO_3)_3 \cdot 9H_2O$ (grade: ACS 99.0–100.2%) and $Co(NO_3)_2 \cdot 6H_2O$ (grade: ACS 98.0–102.0% metal basis) supplied by VWR Chemicals and Alfa Aesar GmbH & Co KG. The nitrate salts were used as provided and no further purifications have been performed. The nitrate solutions were combined in a stoichiometric ratio with respect to the metal ions (i.e., Fe:Co = 2:1), about 50 mg of CNTs were added, and the mixture was treated in an ultrasonication bath for 60 min at room temperature. The mixture was then vacuum-filtered and washed with about 20 ml washing agent of acetone and distilled water with a volumetric ratio of 1:1. Subsequently, the solid residue was dried for 24 h at a temperature of 108 °C and afterwards calcinated under argon flow atmosphere (100 sccm) at a temperature of 500 °C for 4 h to convert the nitrates into the corresponding cobalt ferrite according to the following equation:

$$Co(NO_3)_2(s) + 2Fe(NO_3)_3(s)\ CoFe_2O_4(s) + 8NO_2(g) + 2O_2(g)$$

Commercial $CoFe_2O_4$ nanopowder with a particle size of 30 nm have been obtained by Sigma Aldrich.

2.2. Characterization

The resulting $CoFe_2O_4$@CNT nanocomposite was investigated by scanning electron microscopy (SEM) with a Nova 200 NanoSEM (FEI Company, Hilsboro, Oregon, U.S.) operating at 15 kV, combined with an energy dispersive X-ray (EDX) analyzer (AMETEK, Berwyn, Pennsylvania, U.S.). The SEM sample was prepared by placing a tiny amount of powder sample on carbon tape. Crystal structure analyses were carried out by means of an X'Pert Pro MPD PW3040/60 X-ray diffractometer (XRD, PANalytical, Almelo, Niederlande) with Co Kα radiation ($\lambda = 1.79278$ Å) in reflection geometry at a scanning rate of 0.05° s^{-1} in the 2θ range of 10°–80°. Thermogravimetric analysis (TGA) was performed with an SDT-Q600 (TA instruments, Waters Corporation, Milford, Massachusetts, U.S.). In detail, approximately 5 mg of the material were heated to a temperature of 900 °C with a heating rate of 5 K min^{-1} followed by an isothermal dwelling for 15 min under air atmosphere with a flow rate of 100 ml min^{-1}. The magnetic field dependence of the magnetization at 5 K and 300 K in external magnetic fields up to ± 5T was measured by means of a superconducting quantum interference device (MPMS-XL5 SQUID) magnetometer by Quantum Design (San Diego CA, USA). Transmission electron microscopy (TEM) and high-resolution transmission electron microscopy (HRTEM) measurements were performed using a Tecnai F30 (FEI Company, Hilsboro, Oregon, U.S.) instrument operated at 300 kV. The TEM samples were prepared by adding a few drops of the sample suspension in acetone on a copper grid with a carbon coating on one side.

2.3. Electrochemical measurements

Electrochemical measurements were performed using Swagelok-type cells. Working electrodes were prepared from the active materials as follows [31]. The $CoFe_2O_4$@CNT composite was mixed with 10 wt% of polyvinylidene fluoride (PVDF) in *N*-methyl-2-pyrrolidinone (NMP) and stirred for 24 h before the resulting slurry was applied to copper net current collectors. The $CoFe_2O_4$ nanoparticles were mixed in a mortar with 5 wt% of PVDF and 10 wt % of carbon black in order to enhance electric conductivity, before adding NMP to fabricate the electrode slurry. The as-prepared electrodes were dried in a vacuum oven (80 °C, <10 mbar) over night, pressed at 10 MPa, and dried again. Subsequently, Swagelok-type cells were prepared in a glove box under dry argon with lithium counter electrodes pressed onto nickel plates. Two sheets of fiber glass separator were soaked with 200 µl of a 1 M $LiPF_6$ solution dissolved in a 1:1 mixture of ethylene carbonate and dimethyl carbonate acting as the electrolyte. Cyclic voltammetry (CV) at a scan rate of 0.1 mV s^{-1} and galvanostatic cycling (GCPL) at specific currents of 100 mA g^{-1}, both in the voltage range of 0.01–3.0 V vs. Li/Li^+, were carried out on a VMP3 potentiostat (BioLogic) at 25 °C.

3. Results and discussion

3.1. Morphology and structure

The morphology and geometry of the filling material and its location inside or outside the CNTs were examined by SEM and TEM, as illustrated by the images in Fig. 1. SEM overview images in secondary-electron (SE) mode (a) and back-scattered-electron (BSE) mode (b) for $CoFe_2O_4$@CNT show, that the filling material is distributed along the inner cavity of the hollow CNTs. Different morphologies of the filling particles (spherical, short rods, etc.) have been observed for the ferrites inside the CNTs. These observations also have also confirmed by TEM measurements as shown in Fig. 1(c–f). HRTEM confirms the crystallinity of the core material as highlighted by the appearance of the lattice fringes shown in Fig. 1 (f).

Elemental mapping reveals that Co and Fe are uniformly distributed within the particles/rods (Fig. S1). Line scans along and across the filling confirm the correlation between the Co and Fe concentration which is consistent with the oxide formation. The C and Co–Fe concentration profiles anti-correlate, indicating that the metal is located inside the tube cores. Quantitative analysis of the respective spectra reveals Fe and Co filling material with atomic percentages of 66(2) and 34(2) w%, respectively, thereby confirming the Fe/Co ratio of 2:1 (Table S1).

3.2. Structural characterization

The XRD pattern of the $CoFe_2O_4$@CNT nanocomposite presented in Fig. 2 confirms the presence of $CoFe_2O_4$. In addition to the characteristic peaks of pristine CNT, the pattern exhibits further reflections which agree with reference data for $CoFe_2O_4$ (cubic space group $Fd\bar{3}m$) from the Crystallography Open Database #1533163 [32]. Pronounced peak broadening indicates the presence of nanosized $CoFe_2O_4$ crystallites, whose grain size is estimated to be 20(5) nm by means of the Scherrer equation applied to the Bragg peak at 41.5°. Note, that other contributions to XRD peak broadening have been neglected for this estimate. TGA data of $CoFe_2O_4$@CNT (see the inset of Fig. 2) show a residual mass of 11(1) wt% after heating the compound to 900 °C in air. This mass content is ascribed to $CoFe_2O_4$ particles, which are the only crystalline constituent besides the CNTs, according to the XRD analysis.

The magnetization of $CoFe_2O_4$@CNT measured in external

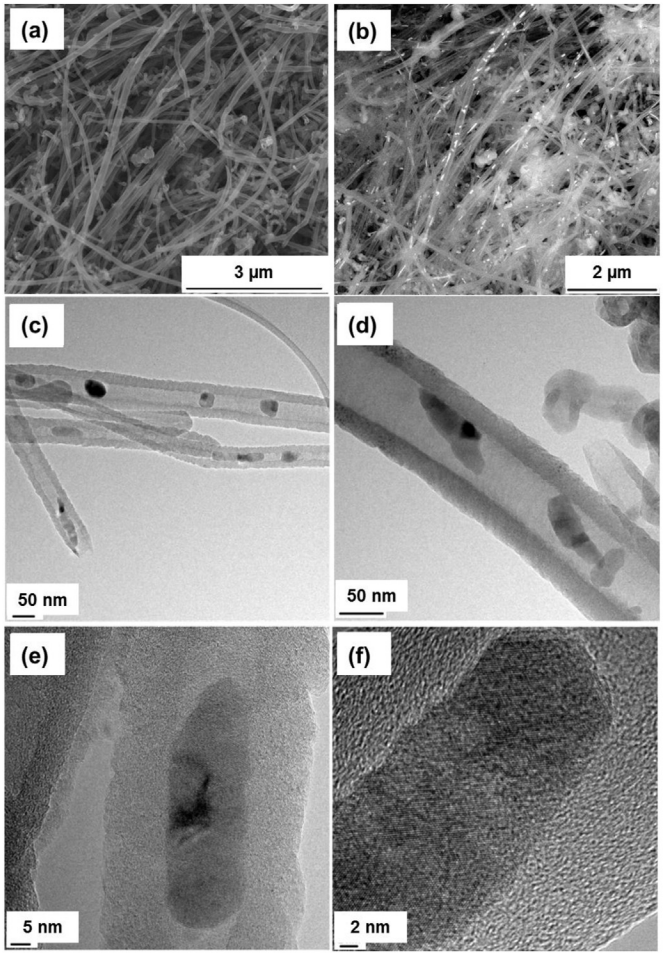

Fig. 1. Electron microscopy images of the $CoFe_2O_4$@CNT nanocomposite by means of (a) SE mode, (b) BSE mode, (c–d) TEM, and (e–f) HRTEM.

magnetic fields up to $\mu_0H = \pm 5$ T is displayed in Fig. 3. Both at temperatures of T = 5 K and 300 K, hysteresis loops with a consistent average saturation magnetization of 1.6 erg G^{-1} g^{-1} are observed. This observation agrees with previous reports of the ferromagnetic behavior of $CoFe_2O_4$ nanoparticles [33,34], where the magnetic properties are found to be highly size-dependent [35–37]. Taking the mass fraction of the $CoFe_2O_4$ in the studied $CoFe_2O_4$@CNT nanocomposite of ~11 wt% into account, the detected saturation magnetization concurs with saturation values of $CoFe_2O_4$ nanoparticles reported in Ref. [37].

3.3. Electrochemical performance

The electrochemical performance of the $CoFe_2O_4$@CNT nanocomposite was studied in comparison to bare $CoFe_2O_4$ nanoparticles by means of CV and GCPL. Fig. 4 shows the 1st, 2nd and 10th cycles of CV measurements for both materials, initially starting with reductive scans at 0.1 mV s^{-1}. For the bare $CoFe_2O_4$ nanoparticles (Fig. 4(a)), in the initial half cycle reduction peaks occur at 1.5 V (R0), 1.1 V, and 0.55 V (R1/SEI) with a shoulder at 0.95 V, before ending in an active range at 0.01 V (R2). In all subsequent reductive half cycles the most pronounced reduction peak occurs at 0.85 V (R1*). While R0 completely vanishes after the first cycle, the intensities of all other reductive features gradually decrease until cycle 10. In all oxidative scans a broad oxidation double peak is observed between 1.5 V and 2.5 V with a maximum intensity

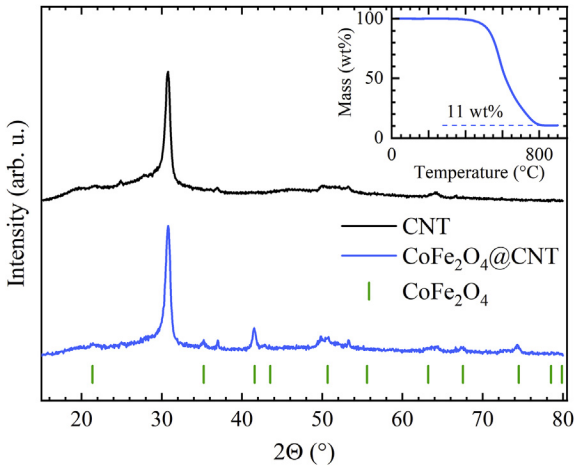

Fig. 2. Powder XRD patterns of $CoFe_2O_4$@CNT and of pristine CNT. Vertical ticks label Bragg positions of bulk $CoFe_2O_4$ (space group $Fd\bar{3}m$) [32]. Inset: TGA data of $CoFe_2O_4$@CNT.

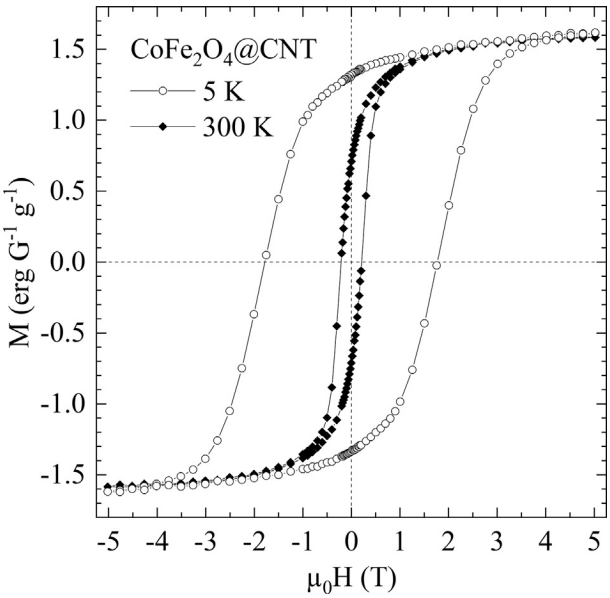

Fig. 3. Magnetization data of $CoFe_2O_4$@CNT, measured in external magnetic fields up to $\mu_0H = \pm 5$ T at constant temperatures of 5 K and 300 K, respectively.

around 1.65 V (O1), which also ceases until cycle 10.

The electrochemical lithium storage in $CoFe_2O_4$ of up to 8 Li^+/f.u. is supposed to follow a conversion mechanism according to Eq. (1), which can be preceded by initial intercalation of Li^+-ions into the original ferrite structure [38]. In the first CV cycle of the $CoFe_2O_4$ nanoparticles, the latter may be indicated by R0. The pronounced reduction peak R1 most likely signals both the conversion to Co and Fe, which leads to an irreversible decomposition of the ferrite starting compound [9,38], and the formation of a solid electrolyte interphase (SEI) [39]. The reductive activity R2 originates from the intercalation of Li^+-ions into the added carbon black [40]. After the reductive decomposition of $CoFe_2O_4$ in the initial half cycle, separate oxidation of Co and Fe to CoO and Fe_2O_3, respectively, at O1 is supposed to take place, followed by the corresponding conversion processes at R1* (Eq. (2)) [1,3,9,10,12,15,18].

$$CoFe_2O_4 + 8\ Li^+ + 8\ e^- \text{ - > } Co + 2\ Fe + 4\ Li_2O \quad (1)$$

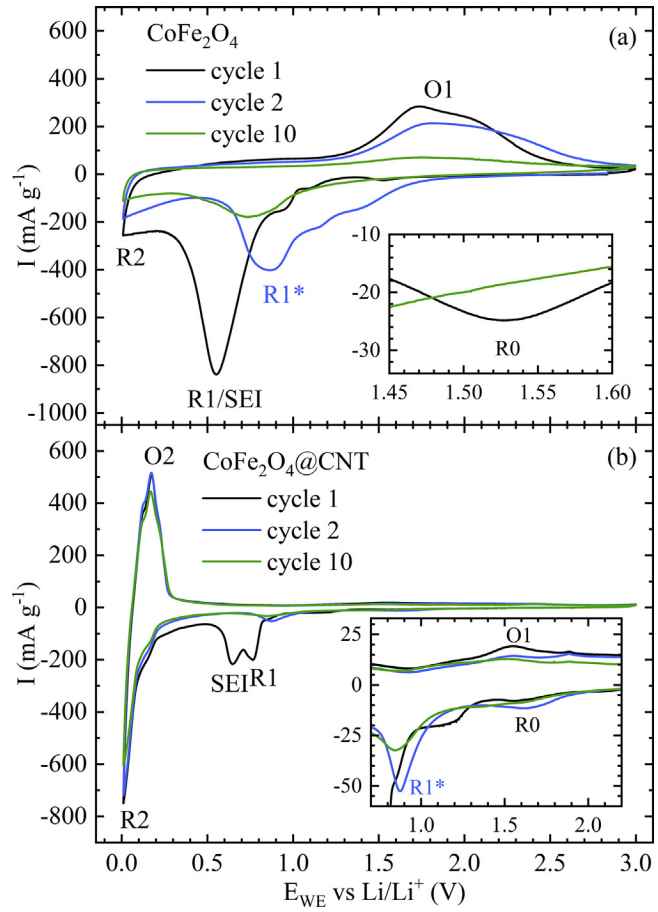

Fig. 4. Cyclic voltammograms of (a) $CoFe_2O_4$ nanoparticles, and (b) $CoFe_2O_4$@CNT obtained at a scan rate of 0.1 mV s^{-1}. R0 to R2 and O1 to O2 label reduction and oxidation features, respectively, as described in the text.

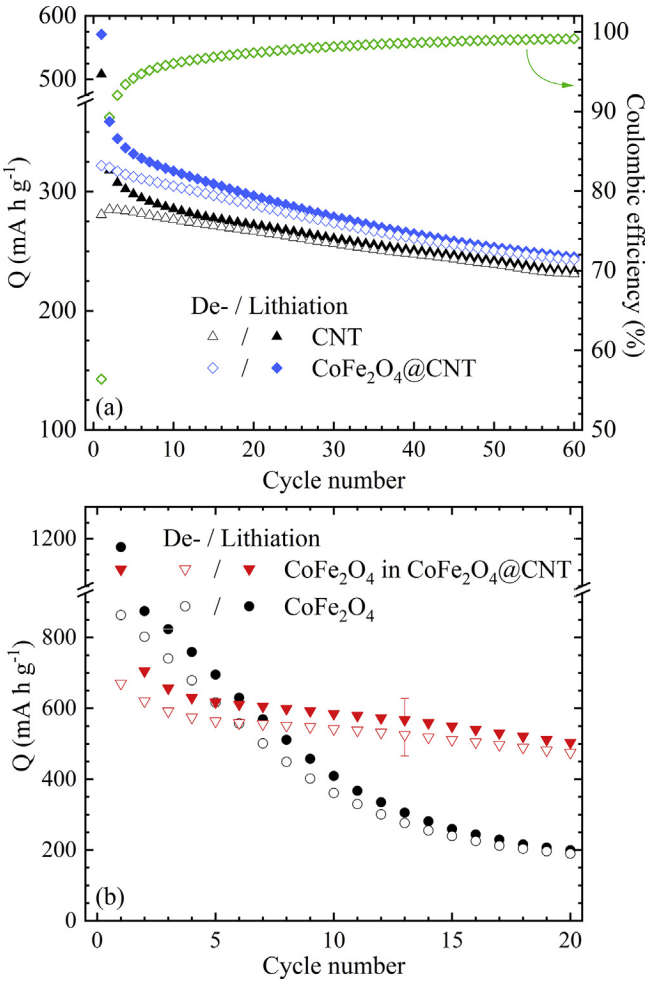

Fig. 5. (a) Dis-/charge capacities at 100 mA g^{-1} of CNTs and $CoFe_2O_4$@CNT as well as corresponding coulombic efficiencies. (b) Capacity contribution of only $CoFe_2O_4$ in $CoFe_2O_4$@CNT and capacities of bare $CoFe_2O_4$ nanoparticles.

$$Co + 2\ Fe + 4\ Li_2O <-> CoO + 2\ Fe_2O_3 + 8\ Li^+ + 8\ e^- \quad (2)$$

The $CoFe_2O_4$@CNT nanocomposite's CV in Fig. 4(b) can be understood considering both the electrochemical response of bare $CoFe_2O_4$ nanoparticles (see Fig. 4(a)) and of pristine CNTs [41–44]. In particular, the redox pair R2/O2 around 0.1 V indicates the intercalation/deintercalation of Li^+-ions between the graphitic layers of the CNTs [45,46]. It seems dominant due to the small mass content of $CoFe_2O_4$ of 11 wt% in the composite material. The reduction peaks attributed to $CoFe_2O_4$ are now observed at 1.6 V (R0), 1.2 V, and 0.7 V (SEI) with a distinct shoulder at 0.8 V (R1) in the initial half cycle, and subsequently at 1.6 V (R0) and 0.9 V (R1*). Reversible oxidation peaks again occur in the range between 1.5 V and 2.0 V reaching maximum intensity around 1.55 V (O1). Generally, compared with the bare $CoFe_2O_4$ nanoparticles, the corresponding reduction and oxidation peaks in $CoFe_2O_4$@CNT appear at slightly higher and lower potentials, respectively. This indicates smaller over potentials and thus improved energy efficiency in the compound. Furthermore, cycling stability is superior, yielding yet noticeable redox activity in the 10th cycle. Both improvements can be attributed to benefits of the CNTs in the $CoFe_2O_4$@CNT composite, i.e., to enhanced overall conductivity and better structural integrity.

Fig. 5(a) shows specific charge and discharge capacities of the $CoFe_2O_4$@CNT nanocomposite and of pristine CNTs, respectively, observed in GCPL measurements at 100 mA g^{-1}. Over the course of 60 dis-/charge cycles the $CoFe_2O_4$@CNT nanocomposite consistently retains higher capacities than the pristine CNTs. In both materials, a large initial discrepancy between charge and discharge capacity of 571/322 mA h g^{-1} and 508/281 mA h g^{-1}, respectively, is to a large extend attributed to SEI formation. However, irreversible capacity losses continuously occur during the first couple of cycles resulting in moderate coulombic efficiencies that in case of the $CoFe_2O_4$@CNT nanocomposite exceed 97% only after the 15th cycle. After 60 cycles 243 mA h g^{-1} can still be discharged from the nanocomposite which corresponds to an overall capacity retention of 76%. The specific contribution of the ferrite nanoparticles to the capacities of the $CoFe_2O_4$@CNT composite are evaluated by subtracting the measured capacities of pristine CNTs, weighted with the mass ratio of 89:11 (CNTs: $CoFe_2O_4$). The resulting capacities of the $CoFe_2O_4$ nanoparticles in $CoFe_2O_4$@CNT are depicted in Fig. 5(b) in comparison to those of bare $CoFe_2O_4$ nanoparticles. The initial charge capacities, 1173 mA h g^{-1} for the nanoparticles and 1103 mA h g^{-1} for the composite, are significantly higher than the theoretical expectation of 914 mA h g^{-1}. This can be attributed to SEI formation at the $CoFe_2O_4$/electrolyte interface. In both cases, there are significant capacity losses upon cycling, which are yet much more severe for the pure $CoFe_2O_4$ nanoparticles. After 20 cycles, the bare nanoparticles' discharge capacity has decreased to 190 mA h g^{-1}, corresponding to a loss of 78% of the initial discharge capacity. In the $CoFe_2O_4$@CNT electrode,

on the other hand, 475 mA h g^{-1}, i.e. 71% of the initial discharge capacity, are retained after 20 cycles, that corresponding to a loss of only 29%. This demonstrates that embedding nano sized $CoFe_2O_4$ in a conductive matrix of carbon by filling it into CNTs can partly compensate for the typical capacity fading associated with the conversion reactions upon electrochemical de-/lithiation known for ferrite materials.

4. Conclusions

$CoFe_2O_4$-filled multi-walled carbon nanotubes have been investigated by means of their lithium storage ability as an anode material for lithium ion batteries. The involved conversion mechanism known for nanosized $CoFe_2O_4$ was confirmed in cyclic voltammetry measurements. In comparison to bare $CoFe_2O_4$ nanoparticles, $CoFe_2O_4$@CNT nanocomposite shows smaller overpotentials and hence improved energy efficiency. We attribute this mainly to enhanced conductivity induced by the linked CNT network. Further, the ferrite's capacity retention over the first 20 dis-/charge cycles is improved from 22% in the pure nanoparticles to 71% in $CoFe_2O_4$@CNT. The data hence demonstrate that embedding nanoparticles inside the protective and conductive shells of CNTs opens a way to utilize high theoretical capacities of $CoFe_2O_4$ and other transition metal oxides for electrochemical energy storage.

Declaration of competing interest

The authors declare that they have no known competing financial interests or personal relationships that could have appeared to influence the work reported in this paper.

CRediT authorship contribution statement

Lucas Möller: Writing - original draft, Investigation, Visualization. **Elisa Thauer:** Writing - original draft, Writing - review & editing, Visualization. **Alexander Ottmann:** Conceptualization, Methodology. **Lukas Deeg:** Investigation. **Rasha Ghunaim:** Visualization. **Silke Hampel:** Conceptualization. **Rüdiger Klingeler:** Conceptualization, Writing - review & editing, Supervision.

Acknowledgements

The authors thank G. Kreutzer for performing the TEM and EDX studies. Financial support by the by Deutsche Forschungsgemeinschaft (DFG) via project KL1824/12 is gratefully acknowledged.

Appendix A. Supplementary data

Supplementary data to this article can be found online at https://doi.org/10.1016/j.jallcom.2020.155018.

References

[1] J. Cabana, L. Monconduit, D. Larcher, M.R. Palacín, Beyond intercalation-based Li-ion batteries: the state of the art and challenges of electrode materials reacting through conversion reactions, Adv. Energy Mater. 22 (2010) E170–E192.
[2] P. Poizot, S. Laruelle, S. Grugeon, L. Dupont, J.-M. Tarascon, S. Laruelle, J.-M. Tarascon, Searching for new anode materials for the Li-ion Searching for new anode materials for the Li-ion technology: time to deviate from the usual path, J. Power Sources 97–98 (2001) 235–239.
[3] P. Poizot, S. Laruelle, S. Grugeon, L. Dupont, J.M. Tarascon, Nano-sized transition-metal oxides as negative-electrode materials for lithium-ion batteries, Nature 407 (2000) 496–499.
[4] G.H. Jonker, Analysis of the semiconducting properties of cobalt ferrite, J. Phys. Chem. Solid. 9 (1959) 165–175.
[5] M. Fichtner, Konversionsmaterialien für die Energiespeicherung, Chem. Unserer Zeit 47 (2013) 230–238.
[6] P.G. Bruce, B. Scrosati, J.-M. Tarascon, Nanomaterials for rechargeable lithium batteries, Angew. Chem. Int. Ed. 47 (2008) 2930–2946.
[7] B. Scrosati, J. Garche, Lithium batteries: status, prospects and future, J. Power Sources 195 (2010) 2419–2430.
[8] X. Fu, D. Chen, M. Wang, Y. Yang, Q. Wu, J. Ma, X. Zhao, Synthesis of porous CoFe2O4 octahedral structures and studies on electrochemical Li storage behavior, Electrochim. Acta 116 (2014) 164–169.
[9] Y.-Q. Chu, Z.-W. Fu, Q.-Z. Qin, Cobalt ferrite thin films as anode material for lithium ion batteries, Electrochim. Acta 49 (2004) 4915–4921.
[10] N. Wang, H. Xu, L. Chen, X. Gu, J. Yang, Y. Qian, A general approach for MFe2O4 (M = Zn, Co, Ni) nanorods and their high performance as anode materials for lithium ion batteries, J. Power Sources 247 (2014) 163–169.
[11] S. Yoon, Facile microwave synthesis of CoFe2O4 spheres and their application as an anode for lithium-ion batteries, J. Appl. Electrochem. 44 (2014) 1069–1074.
[12] Y. Wang, D. Su, A. Ung, J.H. Ahn, G. Wang, Hollow CoFe2O4 nanospheres as a high capacity anode material for lithium ion batteries, Nanotechnology 23 (2012) 55402.
[13] D.H. Deng, H. Pang, J.M. Du, J.W. Deng, S.J. Li, J. Chen, J.S. Zhang, Fabrication of cobalt ferrite nanostructures and comparison of their electrochemical properties, Cryst. Res. Technol. 47 (2012) 1032–1038.
[14] Z.-J. Jiang, S. Cheng, H. Rong, Z. Jiang, J. Huang, General synthesis of MFe2O4/carbon (M = Zn, Mn, Co, Ni) spindles from mixed metal organic frameworks as high performance anodes for lithium ion batteries, J. Mater. Chem. A 5 (2017) 23641–23650.
[15] L. Wu, Q. Xiao, Z. Li, G. Lei, P. Zhang, L. Wang, CoFe2O4/C composite fibers as anode materials for lithium-ion batteries with stable and high electrochemical performance, Solid State Ionics 215 (2012) 24–28.
[16] L. Wang, L. Zhuo, C. Zhang, F. Zhao, Carbon dioxide-induced homogeneous deposition of nanometer-sized cobalt ferrite (CoFe2O4) on graphene as high-rate and cycle-stable anode materials for lithium-ion batteries, J. Power Sources 275 (2015) 650–659.
[17] P.R. Kumar, P. Kollu, C. Santhosh, K. Eswara Varaprasada Rao, D.K. Kim, A.N. Grace, Enhanced properties of porous CoFe2O4 –reduced graphene oxide composites with alginate binders for Li-ion battery applications, New J. Chem. 38 (2014) 3654–3661.
[18] L. Wang, L. Zhuo, H. Cheng, C. Zhang, F. Zhao, Porous carbon nanotubes decorated with nanosized cobalt ferrite as anode materials for high-performance lithium-ion batteries, J. Power Sources 283 (2015) 289–299.
[19] R. Jin, Q. Wang, Y. Cui, S. Zhang, MFe2O4 (M = Ni, Co) nanoparticles anchored on amorphous carbon coated multiwalled carbon nanotubes as anode materials for lithium-ion batteries, Carbon 123 (2017) 448–459.
[20] J. Wang, Z. Dong, J. Huang, J. Li, X. Jin, J. Niu, J. Sun, J. Jin, J. Ma, Filling carbon nanotubes with Ni–Fe alloys via methylbenzene-oriented constant current electrodeposition for hydrazine electrocatalysis, Appl. Surf. Sci. 270 (2013) 128–132.
[21] Y. Liu, H. Jiang, Y. Zhu, X. Yang, C. Li, Transition metals (Fe, Co, and Ni) encapsulated in nitrogen-doped carbon nanotubes as bi-functional catalysts for oxygen electrode reactions, J. Mater. Chem. A 4 (2016) 1694–1701.
[22] M.H. Xu, W. Zhong, X.S. Qi, C.T. Au, Y. Deng, Y.W. Du, Highly stable Fe–Ni alloy nanoparticles encapsulated in carbon nanotubes, J. Alloys Compd. 495 (2010) 200–204.
[23] R. Ghunaim, M. Scholz, C. Damm, B. Rellinghaus, R. Klingeler, B. Büchner, M. Mertig, S. Hampel, Single-crystalline FeCo nanoparticle-filled carbon nanotubes, Beilstein J. Nanotechnol. 9 (2018) 1024–1034.
[24] R. Klingeler, S. Hampel, B. Büchner, Carbon nanotube based biomedical agents for heating, temperature sensoring and drug delivery, Int. J. hyperther. 24 (2008) 496–505, the official journal of European Society for Hyperthermic Oncology, North American Hyperthermia Group.
[25] A. Vyalikh, A.U.B. Wolter, S. Hampel, D. Haase, M. Ritschel, A. Leonhardt, H.-J. Grafe, A. Taylor, K. Krämer, B. Büchner, R. Klingeler, A carbon-wrapped nanoscaled thermometer for temperature control in biological environments, Nanomedicine (London, England) 3 (2008) 321–327.
[26] A. Winkler, T. Mühl, S. Menzel, R. Kozhuharova-Koseva, S. Hampel, A. Leonhardt, B. Büchner, Magnetic force microscopy sensors using iron-filled carbon nanotubes, J. Appl. Phys. 99 (2006) 104905.
[27] Elisa Thauer, Alexander Ottmann, Philip Schneider, Lucas Möller, Lukas Deeg, Rouven Zeus, Florian Wilhelmi, Lucas Schlestein, Christoph Neef, Rasha Ghunaim, Markus Gellesch, Christian Nowka, Maik Scholz, Marcel Haft, Sabine Wurmehl, Karolina Wenelska, Ewa Mijowska, Aakanksha Kapoor, Ashna Bajpai, Silke Hampel, Rüdiger Klingeler, Filled carbon nanotubes as anode materials for Lithium-ion batteries, Molecules 25 (2020) 1064, https://doi.org/10.3390/molecules25051064.
[28] A. Ottmann, M. Scholz, M. Haft, E. Thauer, P. Schneider, M. Gellesch, C. Nowka, S. Wurmehl, S. Hampel, R. Klingeler, Electrochemical Magnetization Switching and Energy Storage in Manganese Oxide filled Carbon Nanotubes, Sci. Rep. 7 (2017), 13625, https://doi.org/10.1038/s41598-017-14014-7.
[29] Nan Yan, Xuhui Zhou, Yan Li, Fang Wang, Hao Zhong, Hui Wang, Qianwang Chen, Fe_2O_3 Nanoparticles Wrapped in Multi-walled Carbon Nanotubes With Enhanced Lithium Storage Capability, Sci. Rep. 3 (2013), 3392. https://doi.org/10.1038/srep03392.
[30] S. Al Khabouri, S. Al Harthi, T. Maekawa, Y. Nagaoka, M.E. Elzain, A. Al Hinai, A.D. Al-Rawas, A.M. Gismelseed, A.A. Yousif, Composition, electronic and

magnetic investigation of the encapsulated ZnFe2O4 nanoparticles in multi-wall carbon nanotubes containing Ni residuals, Nanoscale res.lett. 10 (2015) 262.
[31] A. Ottmann, G.S. Zakharova, B. Ehrstein, R. Klingeler, Electrochemical performance of single crystal belt-like NH4V3O8 as cathode material for lithium-ion batteries, Electrochim. Acta 174 (2015) 682–687.
[32] T.A.S. Ferreira, J.C. Waerenborgh, M.H.R.M. Mendonça, M.R. Nunes, F.M. Costa, Structural and morphological characterization of FeCo2O4 and CoFe2O4 spinels prepared by a coprecipitation method, Solid State Sci. 5 (2003) 383–392.
[33] S. Sun, H. Zeng, D.B. Robinson, S. Raoux, P.M. Rice, S.X. Wang, G. Li, Monodisperse MFe2O4 (M = Fe, Co, Mn) nanoparticles, J. Am. Chem. Soc. 126 (2004) 273–279.
[34] S. Ayyappan, S. Mahadevan, P. Chandramohan, M.P. Srinivasan, J. Philip, B. Raj, Influence of Co2+ ion concentration on the size, magnetic properties, and purity of CoFe2O4 spinel ferrite nanoparticles, J. Phys. Chem. C 114 (2010) 6334–6341.
[35] Sorensen Tang, Hadjipanayis Klabunde, Size-dependent Curie temperature in nanoscale MnFe2O4 particles, Phys. Rev. Lett. 67 (1991) 3602–3605.
[36] Q. Song, Z.J. Zhang, Shape control and associated magnetic properties of spinel cobalt ferrite nanocrystals, J. Am. Chem. Soc. 126 (2004) 6164–6168.
[37] M. Grigorova, H.J. Blythe, V. Blaskov, V. Rusanov, V. Petkov, V. Masheva, D. Nihtianova, L.M. Martinez, J.S. Muñoz, M. Mikhov, Magnetic properties and Mössbauer spectra of nanosized CoFe2O4 powders, J. Magn. Magn Mater. 183 (1998) 163–172.
[38] P. Lavela, G.F. Ortiz, J.L. Tirado, E. Zhecheva, R. Stoyanova, S. Ivanova, High-performance transition metal mixed oxides in conversion electrodes: a combined spectroscopic and electrochemical study, J. Phys. Chem. C 111 (2007) 14238–14246.
[39] P. Verma, P. Maire, P. Novák, A review of the features and analyses of the solid electrolyte interphase in Li-ion batteries, Electrochim. Acta 55 (2010) 6332–6341.
[40] R. Gnanamuthu, C.W. Lee, Electrochemical properties of Super P carbon black as an anode active material for lithium-ion batteries, Mater. Chem. Phys. 130 (2011) 831–834.
[41] B.J. Landi, M.J. Ganter, C.D. Cress, R.A. DiLeo, R.P. Raffaelle, Carbon nanotubes for lithium ion batteries, Energy Environ. Sci. 2 (2009) 638–654.
[42] de las Casas, W. Li Charles, A review of application of carbon nanotubes for lithium ion battery anode material, J. Power Sources 208 (2012) 74–85.
[43] A. Varzi, C. Täubert, M. Wohlfahrt-Mehrens, M. Kreis, W. Schütz, Study of multi-walled carbon nanotubes for lithium-ion battery electrodes, J. Power Sources 196 (2011) 3303–3309.
[44] A. Ottmann, M. Scholz, M. Haft, E. Thauer, P. Schneider, M. Gellesch, C. Nowka, S. Wurmehl, S. Hampel, R. Klingeler, Electrochemical magnetization switching and energy storage in manganese oxide filled carbon nanotubes, Sci. Rep. 7 (2017) 13625.
[45] S.Y. Chew, S.H. Ng, J. Wang, P. Novák, F. Krumeich, S.L. Chou, J. Chen, H.k. Liu, Flexible free-standing carbon nanotube films for model lithium-ion batteries, Carbon 47 (2009) 2976–2983.
[46] Z. Xiong, Y. Yun, H.-J. Jin, Applications of carbon nanotubes for lithium ion battery anodes, Materials 6 (2013) 1138–1158.